Biochemical Engineering Journal 23 (2005) 123–130

Biochemical Engineering Journal

www.elsevier.com/locate/bej

Effects of adding inert spheres into the filter bed on the performance of biofilters for gaseous toluene removal

Xi Jin-Ying, Hu Hong-Ying*, Zhu Hong-Bo, Qian Yi

ESPC, Department of Environmental Science and Engineering, Tsinghua University, Beijing 100084, China

Received 14 June 2004; accepted 29 October 2004

Abstract

To investigate the effect of adding large size inert materials into natural organic packing media in waste gas treatment, two biofilters, one packed with buckwheat hulls and inert spheres and the other packed with buckwheat hulls only, were used in parallel experiments to treat toluene gas for 305 continuous days. The toluene removal capacities and pressure drops of the two biofilters were compared during the experiments. The physical properties of the filter beds were also investigated by pulse injection technique combined with a mathematical model. In the late phase of the operation with a sufficient supply of nutrients, the biofilter with inert spheres showed a higher toluene removal capacity than the biofilter without inert spheres. This was due to the fact that the biofilter with inert spheres had less bed compaction and a greater increase in specific surface area. The pressure drop of the biofilter with inert spheres was also significantly lower and more stable than that of the biofilter without inert spheres due to its higher bed void fraction. All the experimental results quantitatively showed that adding inert spheres into the filter beds could improve the performance of the biofilter under long-term operation.

Keywords: Biofilter; Bed compaction; Inert spheres; Pressure drop; Toluene gas

1. Introduction

Over the past two decades, different techniques, such as incineration, catalytic oxidation, adsorption and biological treatment have been developed to control pollution from volatile organic compounds (VOCs) [1]. Compared with other techniques, biological treatment is more often used for low concentration VOCs treatment (<3000 mg m^{-3} generally) and has advantages of simple configuration, low capital and operation costs and minimum secondary pollution production [2–4]. Biofilters are the earliest type of biological reactor and many scientists and technical engineers focused on them [5].

The characteristics and functions of the packing media are very important for biofilters to perform well. An ideal packing medium should meet the following requirements [6,7]: (1) it is easy to maintain optimum conditions, such as high moisture content, sufficient nutrients and suitable pH for microbial growth in the packing medium; (2) it should have large surface area and uniform pore distribution to gain high VOC mass-transfer efficiency from the gas phase to the packing media; (3) it should have low pressure drops to reduce energy consumption; (4) it should have minimum bed compaction and deterioration to avoid frequent replacement; (5) it should be cheap and easy to obtain.

Packing media used for waste gas biofiltration are usually divided into two categories: natural organic packing media and inert packing media. The natural organic packing media, such as compost, peat, soil and wood chips, have been the most frequently used from the early period of the application, especially for conventional biofilters with open beds. The advantage of natural organic packing media is that they are usually cheap, comprising some nutrients and active microorganisms, and thus make the biofilter to have a quick startup. Nevertheless, bed compaction often occurs for natural organic packing media after a period of operation, which can lead to a significant bed pressure drop, channeling, the

* Corresponding author. Tel.: +86 10 62794005; fax: +86 10 62771472.
E-mail address: hyhu@tsinghua.edu.cn (Hu Hong-Ying).

1369-703X/$ – see front matter © 2004 Elsevier B.V. All rights reserved.
doi:10.1016/j.bej.2004.10.013

formation of anaerobic zones and decreased long-term operation performance. In recent years, more and more inert packing media, including perlite, ceramic, activated carbon, lava rocks and many artificial plastic or glass packing media have been studied by researchers and applied by companies. For inert packing media, its advantages are that it is physically intensive and chemically stable, having minimum bed compaction and a longer lifetime. However, most inert and synthetic packing media are more expensive than natural organic packing media [8]. Many researchers have reported that in order to minimize the bed compaction and extend the lifetime of the organic packing media, adding large size inert materials, such as glass beads, polystyrene spheres and lava rocks, into the organic packing media could decrease the bed compaction and avoid clogging and significant pressure drop [9–11]. Nevertheless, most of these works did not report how the addition of large size inert materials into the filter bed would affect the VOC removal capacity of the biofilters quantitatively. There are almost no reports of any systematic comparison of biofilters with and without inert materials under long-term operation in the literature.

To predict how adding inert materials will affect the VOC-removal capacity of a biofilter, the change of the physical properties of the filter beds should be considered. Pellet size and the specific surface area of the filter bed are the key physical properties that influence the VOC mass transfer rate and removal rate. They were found to be the major factors limiting the compost-based biofilters' VOCs removal capacity [12]. The addition of large size inert material reduces the specific surface area of the filter bed and then may lead the VOC removal rate to decrease. On the other hand, adding inert materials prevents the bed compaction and maintains the effective length of the filter bed, which may also affect the VOC removal rate. Thus, the effect of adding inert materials on physical properties and bed compaction should also be studied for long periods of operation.

The aim of this study is to investigate the effect of adding inert materials into the filter bed on the biofilter's VOC removal performance under long-term operation. The filter bed's physical properties, the VOC removal capacities, bed compaction and pressure drops of two biofilters with and without inert spheres were compared.

2. Materials and methods

2.1. Biofiltration systems

Two paralleled biofilter systems, identified as BF1 and BF2, were established (Fig. 1). The biofilters had same setup; each biofilter column had a height of 1.5 m and an inner diameter of 0.1 m. The filter bed was divided equally into four layers, which were identified as layers A, B, C and D from the bottom to the top of the biofilter. The overall volume of the filter bed was 7.9 L for each biofilter.

Buckwheat hulls were used as the organic packing medium as reported in a previous study [13]. The inert material selected here was polypropylene spheres (Fig. 1). BF1 was packed with 0.90 kg buckwheat hulls, which had an average diameter of 5 mm, a bulk density of 130 kg m^{-3} and a moisture content of 10%. The void fraction of the BF1 bed was 0.65. BF2 was packed with 0.71 kg buckwheat hulls mixed with 0.43 kg polypropylene spheres, which had a diameter of 25 mm and a bulk density of 118 kg m^{-3}. The void fraction of the BF2 bed was 0.72.

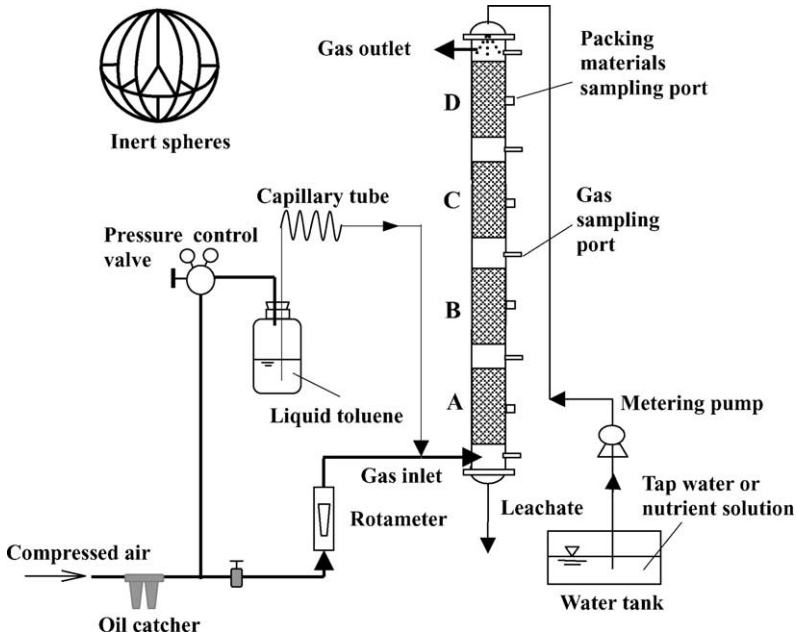

Fig. 1. The schematic of the biofilter system and the inert spheres used in this study.

Toluene was selected as the representative VOC, because it is a very typical and widely used chemical in many industrial areas. To produce a toluene gas with the desired concentration, a toluene feeding apparatus was set up using a capillary tube made of quartz glass (Yongnian Corp., China). The flow rate of liquid toluene fed into the influent air was controlled by setting the proper radius, length and inlet pressure of the capillary. The functional relationship can be described by Poiseuilli's equation:

$$Q = \frac{\pi R^4}{8\eta L}(P_1 - P_2) \quad (1)$$

where Q ($m^3\,s^{-1}$) is the flow rate of liquid in the capillary tube; R (m) the capillary radius, L (m) the capillary length, η (Pa s) the viscosity of the liquid, P_1 (Pa) the inlet pressure of the capillary tube and P_2 (Pa) is the outlet pressure of the capillary tube. A capillary with a length of 40 m and an inner diameter of 250 μm was used here, and the value of P_1 was about 3.0×10^4 Pa.

A metering pump (Iwaki EHC-R220C, Japan) was used to send tap water or a nutrients solution from a stock tank to the filter bed.

2.2. Operating conditions and experimental control

After the biofilters were inoculated with 1.2 L activated sludge (MLSS = 6.3 g L^{-1}) taken from a wastewater treatment plant, biofilters BF1 and BF2 were operated continuously in parallel for 305 days. After day 305, the pressure drop of BF1 became so high that the biofilter could not continue to run, while BF2 had a relatively constant pressure drop and could run through the end of the experiment on day 360. The operating conditions of the two biofilters were kept the same, and are shown in Table 1. To compare the performance of the biofilters under nutrient-rich and nutrient-limited conditions, the whole experimental period was divided into four phases according to different spray conditions. During Phase I (days 1–45) and Phase III (days 136–210), tap water was sprayed into the filter bed directly, while during Phase II (days 46–135) and Phase IV (days 211–305 for BF1, days 211–360 for BF2), nutrient solution was used. The nutrient solution contained 10 g L^{-1} of $NaNO_3$, 0.7 g L^{-1} of Na_2HPO_4 and 0.6 g L^{-1} of NaH_2PO_4.

Table 1
Operating conditions of the biofilters

Environment	
Temperature	19–28 °C
Relative humidity	50–85%
Gaseous toluene feeding	
Inlet toluene concentration	200–400 mg m^{-3}
Flow rate	0.5 $m^3\,h^{-1}$, upflow
Empty bed retention time	1 min
Velocity	64 m h^{-1}
Loading rate	10–25 g toluene $m^{-3}\,h^{-1}$
Spraying	
Sprayed liquid	Tap water or nutrient solution
Spraying intervals	Once every 6 h
Quantity sprayed	200–300 mL d^{-1}

During the experiment period, the concentrations of gaseous toluene in the inlets and outlets of the two biofilters, the microbial concentration in the packing medium, and the length and the pressure drop of the filter bed were monitored at intervals. The pulse injection technique was also applied on different days in order to investigate changes in the filter beds' physical properties.

2.3. Molecular retention time distribution curve analysis

The pulse injection technique is often used to monitor the flow behavior in reactors by using an Axial Dispersion Model [14,15]. The tracers used to estimate the retention time of the gas flow in biofilters should be strictly hydrophobic to avoid a mass-transfer process between the gas phase and the packing medium. Unlike the normal pulse injection technique, an absorbable tracer was used here. The time course of the tracer concentration in the outlet of the biofilter, which could be define as the molecular retention time distribution (MRTD) curve [16], was used to analyze the physical properties of the filter bed. The difference between using a hydrophobic tracer (for example methane) and an absorbable tracer was well interpreted in Mendoza's work [17].

The 1,2-dichloroethane (DCE) was selected as the absorbable tracer because it is non-degradable in the biofilter. Under the superficial velocity of 64 m h^{-1}, 0.5 g DCE was injected into the inlet of the biofilter and the DCE concentration in the outlet was measured at intervals to gain the MRTD curve. The sampling of the outlet gas continued until the DCE concentration was lower than 1% of the peak concentration. The recoveries of the DCE were between 0.91 and 0.96 in most cases.

To characterize the MRTD curves, the theoretical moments ν_1 and μ_2 of the MRTD curve were then calculated. ν_1 (s) is the first absolute moment of the MRTD curve, which represents the average molecular retention time of the VOC pulse. μ_2 (s^2) is the second moment of the MRTD curve which represents the width of the MRTD curve ν_1 and μ_2 are defined as:

$$\nu_1 = \frac{\int_0^\infty t c_t \mathrm{d}t}{\int_0^\infty c_t \mathrm{d}t} \cong \frac{\sum t_i c_i \Delta t_i}{\sum c_i \Delta t_i} \quad (2)$$

and

$$\mu_2 = \frac{\int_0^\infty (t-\nu_1)^2 c_t \mathrm{d}t}{\int_0^\infty c_t \mathrm{d}t} \cong \frac{\sum (t_i-\nu_1)^2 c_i \Delta t_i}{\sum c_i \Delta t_i} \quad (3)$$

where t (s) is the time after injection and c_t (mg m^{-3}) the outlet gaseous concentration of inert VOC at time t. So, the MRTD curve can be expressed as c_t–t; t_i (s) is the specified time and c_i (mg m^{-3}) is the outlet tracer concentration measured at time t_i. Δt_i (s) is the difference between t_i and t_{i-1}. With the theoretical moments of the MRTD curve, the

physical properties of the filter beds were then analyzed by a newly designed mathematical model, which is described in the latter part of this paper.

2.4. Analytical methods

The concentrations of toluene and 1,2-dichloroethane were analyzed by a gas chromatograph (Shimadazu, GC-14B, Japan) with an FID detector and a capillary column (ULBON HR-10.25 mm × 30 m). Nitrogen was selected as the carrier gas, while pure hydrogen and air were supplied to the FID detector. The temperatures of the column oven, injector and detector were 100, 150 and 150 °C, respectively. A fifty-milliliter gas sample was taken from the biofilter using a glass syringe with a latex seal. A 250-μL gastight syringe (Hamilton Corp., USA) was used to draw fifty microliters of gas from the glass syringe and to inject the gas into the gas chromatograph.

To measure the microbial concentration in the packing medium, the microorganisms or the biolayers existing on the surface of the packing medium were washed out first. About 5 mL of packing medium was taken from the filter bed and put into 50 mL distilled water. After the packing medium was surged by ultrasonic wave (40 kHz, 100 W, 45 s), the microorganisms in the packing medium were washed out of the inert particles into the water. The optical density of the microbial suspension was then measured at a wavelength of 600 nm. In a previous work [18], the relationship between 600 nm optical density of the microbial suspension (OD_{600}, cm^{-1}) and the microbial concentration in the suspension (X_s, expressed as g cell L^{-1} suspension) was discovered to be $X_s = 0.30 \times OD_{600}$. The microbial concentration in the packing medium (X_p, expressed as g cell L^{-1} packing medium) was then calculated by $X_p = X_s \times 50/V_p$, in which V_p is the volume of the packing medium sample in milliliters.

The pressure drop of the filter bed was monitored by a water manometer. The void fraction of the filter bed was measured using the water displacement method as described in the literature [15].

3. Results and discussion

3.1. Toluene removal performance

The toluene removal efficiencies (RE_{tol}) and toluene removal rates ($-r_{tol}$) of BF1 and BF2 are shown in Fig. 2. The data describe the results of about one year's continuous operation.

In Phase I, the RE_{tol} of BF1 and BF2 both increased soon after the startup and then fell to less than 20%. The decrease in RE_{tol} was mainly due to the lack of inorganic nutrients. Many studies reported that inorganic nutrients including nitrogen and phosphorous salts are necessary for maintaining the toluene removal capacity [19,20]. Although organic packing media, such as compost often originally contained some

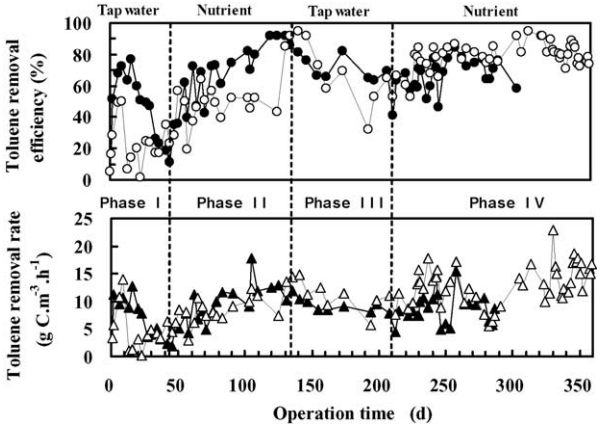

Fig. 2. Variations of the toluene removal efficiency and toluene removal rate for BF1 and BF2: (●) RE_{tol} of BF1; (○) RE_{tol} of BF2; (▲) $-r_{tol}$ of BF1 and (△) $-r_{tol}$ of BF2.

nutrients, these nutrients would be used up after a certain period. During the experiments, tap water was used for spraying in Phases I and III, while a nutrient solution was used in Phases II and IV. As a result, the RE_{tol} of BF1 and BF2 increased in Phases II and IV, but decreased in Phases I and III. This result indicates that a sufficient nutrient supply is very necessary for maintaining the biofilter's toluene removal capacity.

In Phases II and IV with nutrient feeding, the toluene removal capacities of the two biofilters were compared by using the average values of RE_{tol} and $-r_{tol}$. In Phase II, BF1's average RE_{tol} was 67% and its average $-r_{tol}$ was 9.6 g C m^{-3} h^{-1}, which was higher than BF2's average RE_{tol} (51%) and average $-r_{tol}$ (8.8 g C m^{-3} h^{-1}). But in Phase IV, BF1 had an average RE_{tol} of 70% and an average $-r_{tol}$ of 8.1 g C m^{-3} h^{-1}, which was lower than BF2's average RE_{tol} (81%) and $-r_{tol}$ (13.1 g C m^{-3} h^{-1}). The differences of the toluene removal capacity between the two biofilters suggest that adding inert spheres into the filter beds changed some properties of the filter beds.

After day 305, BF1 was seriously clogged and its operation was stopped, while BF2 continued to run under the same conditions until day 360. The toluene removal efficiency of BF2 remained around 80% and did not fall. This result suggests that if the nutrient supply is sufficient, the biofilter with inert spheres can achieve higher and more stable toluene removal capacity throughout a long period of operation.

3.2. Microbial concentrations in the packing medium

The biological removal of toluene is accomplished by the microbial consortium in the packing medium. Thus, the microbial concentrations in the packing medium must be one of important factors affecting the toluene removal capacity. The microbial concentrations in the packing medium of BF1 and BF2 were measured intermittently and the results are shown in Table 2.

Table 2
The microbial concentration in different layers of BF1 and BF2

	Phases											
	I[a]				II			III	IV			
	5 days	12 days	19 days	33 days	47 days	64 days	105 days	194 days	216 days	246 days	250 days	291 days
BF1 (g cell L^{-1})												
Layer A	0.85	1.07	1.23	0.49	0.98	1.02	2.45	2.23	2.06	0.83	1.19	2.19
Layer B	0.92	0.95	0.85	0.47	0.79	–[b]	–	–	–	–	–	–
Layer C	1.25	1.35	0.69	0.58	0.90	0.62	2.54	2.01	1.65	0.77	0.61	0.89
Layer D	1.58	1.26	1.20	0.58	0.90	–	–	–	–	–	–	–
Average	1.15	1.16	0.99	0.53	0.89	0.82	2.50	2.12	1.86	0.80	0.90	1.54
BF2 (g cell L^{-1})												
Layer A	0.76	2.33	0.63	0.60	–	0.68	2.56	0.82	1.24	1.35	2.99	2.15
Layer B	0.86	1.04	1.20	0.59	–	–	–	–	–	–	–	–
Layer C	0.78	0.87	0.71	0.59	–	0.91	0.96	0.90	1.37	1.74	1.47	0.90
Layer D	1.06	0.76	1.23	0.75	–	–	–	–	–	–	–	–
Average	0.86	1.25	0.94	0.63	–	0.79	1.76	0.86	1.30	1.54	2.23	1.53

[a] The microbial concentration on day 0 was calculated to be around 0.85 g cell L^{-1} based on the amount of activated sludge inoculated.
[b] Not measured.

The samples taken from different layers differed by their microbial concentration, indicating that the microbial concentration in the filter bed is not homogeneous. The microbial concentrations in the inlet layer are often higher than in the other layers because the toluene concentration and removal rate are higher in the inlet layer [21,22]. Therefore, the average value of samples from different layers was used to evaluate the microbial concentration in the whole filter bed. For both biofilters, the average microbial concentrations showed variation trends that were almost the same as the changes in the toluene removal efficiency. The average microbial concentration of BF1 in Phase II was higher than that of BF2, which explains the difference of toluene removal capacity between BF1 and BF2 in Phase II. However, the average microbial concentration of BF1 was a little higher than that of BF2 at the beginning and the end of Phase IV, while the toluene removal capacity of BF1 was lower than that of BF2. This indicated that the microbial concentration was not the only reason for the difference in the treatment performance of the two biofilters.

3.3. Bed compaction

During the operation period, the lengths of the filter beds for BF1 and BF2 were monitored, and Fig. 3 shows the percentages of the filter bed length to the initial length. Serious compaction occurred in BF1, and its bed length was only 67% of the initial length by the end of the operation. For BF2, which had inert spheres, the bed compaction was not significant, and the bed length remained 91%. Four layers of each biofilter had almost the same bed length reduction, except for the layer with direct spray, which showed a little more compaction during the operation period (data not shown).

The bed compaction of the filter bed was estimated to be mainly caused by the deterioration of the buckwheat hulls. The particles of the buckwheat hulls decreased in size and cracked more easily due to the effect of biodegradation. The direct water spray also promoted bed compaction, but its effect was very limited. The inert and rigid spheres added into the filter bed could function as a framework which could support the cracked particles and effectively prevent bed compaction.

Bed compaction reduced the effective volume of the filter bed. If the amount of toluene removed by unit volume of filter bed did not change much, the total amount of toluene removed by the whole reactor would be reduced due to bed compaction. In Phase II, since the difference between BF1's bed length and BF2's bed length was not significant (the BF1's bed length was about 90% of the BF2's bed length), the higher microbial concentration in BF1 resulted in BF1 having a higher RE_{tol} and $-r_{tol}$. But in Phase IV, the bed length of BF1 was only about 75% of the BF2's bed length. This resulted in BF1 having a lower RE_{tol} and $-r_{tol}$.

3.4. Analysis of the physical properties of the filter beds

The differences in the toluene removal behabior between BF1 and BF2 should be originally caused by the difference in

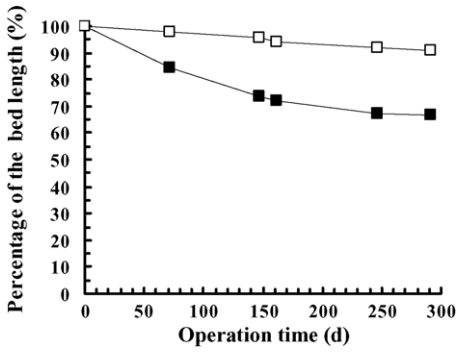

Fig. 3. Variations of the percentage of filter bed length to the initial length: (■) BF1 and (□) BF2.

physical properties of the filter beds. MRTD curves of DCE were used in this study to analyze the physical properties of the filter beds. A math model describing the movement and transfer of DCE in the filter bed was also designed to discover the relationship between the physical properties of the filter beds and the theoretical moments of the MRTD curve.

Some simplifying assumptions were made in order to make the model simple and easy to resolve. These assumptions have also been used in other works [23,24]: (1) the packing medium can be taken as a two-phase system: the air phase and the solid phase. The solid phase includes the inert particles and the biolayers around the particles. (2) The filter bed composition (e.g., void fraction and specific surface area) is homogeneous. (3) The gas phase and solid phase DCE concentrations along the filter bed are mainly decided by convection in the gas phase and adsorption between the gas phase and the solid phase, and the axis diffusion in the gas phase is negligible. (4) The adsorption equilibrium relation between the gas phase concentration and the solid phase concentration can be written in a linear expression.

Accounting for the mass balance in the gas phase, the variation of the DCE concentration in the gas phase is dominated by the convection in the gas phase and the DCE transfer from the gas phase to the solid phase. So, the following equation can be gained:

$$\varepsilon\frac{\partial c_g}{\partial t} = -u\frac{\partial c_g}{\partial x} - \frac{aD_b(Kc_g - c_b)}{\delta_b}, \tag{4}$$

where c_g (mg m^{-3}) is the gas phase DCE concentration, c_b (mg m^{-3}) the average DCE concentration in the solid phase, ε (dimensionless) the void fraction of the filter bed, u (m h^{-1}) the superficial velocity, a (m^2 m^{-3}) the specific surface area in the packing medium, D_b (m^2 h^{-1}) the effective diffusion coefficient for DCE and δ_b (m) is the average thickness of the solid phase. aD_b/δ_b (h^{-1}) represents the overall mass-transfer coefficient from the gas phase to the solid phase. K (dimensionless) is the ratio of the solid phase DCE concentration and the gas phase DCE concentration in the state of equilibrium, x (m) the distance along the filter bed, and t (h) is time.

$\varepsilon(\partial c_g/\partial t)$ represents the variation of DCE in the gas phase, $u(\partial c_g/\partial x)$ represents the convection rate, and $aD_b(Kc_g - c_b/)/\delta_b$ represents the mass-transfer rate from the gas phase to the solid phase.

Accounting for the mass balance in the solid phase, the variation of the DCE concentration in the solid phase is dominated by the transfer process from the gas phase to the solid phase. So another equation is given:

$$\varepsilon_b\frac{\partial c_b}{\partial t} = \frac{aD_b}{\delta_b}(Kc_g - c_b), \tag{5}$$

where ε_b (dimensionless) is the ratio of the solid phase volume to the whole filter bed volume. ε and ε_b have the following relationship:

$$\varepsilon + \varepsilon_b = 1. \tag{6}$$

For DCE pulse input, the initial conditions for this model are as described below.

$$c_{g,t=0} = 0 \tag{7}$$

$$c_{b,t=0} = 0 \tag{8}$$

$$c_{g,x=0} = m\delta(t), \tag{9}$$

where m (mg) is the amount of DCE injected into the inlet of the biofilter, and $\delta(t)$ is the Dirac δ function, which describes the pulse [25]. Eqs. (7) and (8) indicate that the initial gas phase and solid phase DCE concentrations are zero.

By solving the equations in the Laplace domain, the theoretical moments of the MRTD curves can be expressed by the characteristic parameters of the filter bed as shown in Eqs. (10) and (11).

$$\nu_1 = \frac{L}{u}[\varepsilon + (1-\varepsilon)K] \tag{10}$$

$$\mu_2 = \frac{2L}{u}(1-\varepsilon)^2\left(\frac{aD_b}{\delta_b}\right)^{-1}K, \tag{11}$$

where L is the bed length of the biofilter. The characteristic parameters K and aD_b/δ_b can be expressed by the theoretical moments of the MRTD curve as follows:

$$K = \frac{L\varepsilon - \nu_1 u}{L(\varepsilon - 1)} \tag{12}$$

$$\frac{aD_b}{\delta_b} = 2\frac{L\varepsilon^2 - L\varepsilon - \varepsilon\nu_1 u + \nu_1 u}{\mu_2 \mu}. \tag{13}$$

Fig. 4 shows an example of MRTD curves. Using Eqs. (2) and (3), the average molecular retention time (ν_1) and the width of the MRTD curve (μ_2) were calculated based on the MRTD curves. The results are shown in Table 3. The values of ν_1 were from 10 to 15 min, which was much longer than the hydrodynamic empty bed retention time of the two biofilters (about 1 min) by an order of magnitude. This was caused by the adsorption and desorption process of DCE between the gas phase and the packing medium.

As shown in Table 3, the average retention time ν_1 of BF1 decreased and remained only 64% of the initial level at the end of the operation period, while the ν_1 of BF2 kept fairly constant and remained at 88% of the initial level. According to Eq. (10), the value of ν_1 was determined by the bed

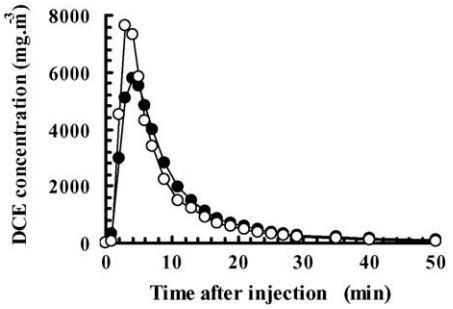

Fig. 4. MRTD curves c_t–t on day 147: (●) BF1 and (○) BF2.

Table 3
Theoretic moments calculated from the MRTD curves

	Time (d)					
	0	72	147	162	246	291
$\nu 1$ (min)						
BF1	15.9	16.6	10.6	14.4	9.7	11.0
BF2	11.6	–	9.1	9.3	10.8	9.5
μ_2 (min^2)						
BF1	116.2	115.9	86.6	109.3	60.5	60.6
BF2	98.9	–	71.3	79.3	59.7	43.1

length L, void fraction ε, superficial velocity u, and equilibrium constant K. The decrease in ν_1 for BF1 was estimated to be caused by the bed length reduction due to compaction. The initial value of ν_1 for BF1 was much higher than that of BF2, while the initial bed lengths of BF1 and BF2 had no difference (see Table 3; Fig. 3). This was due to the fact that the initial void fraction of BF1 was less than that of BF2.

The parameters K and aD_b/δ_b calculated from the theoretical moments of the different days are shown in Fig. 5. As shown in Fig. 5, the K values of BF1 and BF2 were very close and remained steady throughout the operation period. This result indicated that the equilibrium constants of BF1 and BF2 had no significant difference.

In Phases I and II, the aD_b/δ_b value of BF1 was about 5.0–5.5 h^{-1}, while the aD_b/δ_b value for BF2 was between 3.5 and 4.0 h^{-1}, which was lower than that of BF1. Since the values of D_b andδ_b are fairly constant for a specific biofilter and a specific VOC, this difference in the aD_b/δ_b value was most probably due to the fact that the specific surface area of BF1 was higher than that of BF2, which had large size inert spheres. A higher specific surface area improved the mass-transfer and biodegradation rate in the filter beds, resulting in more biomass production and accumulation in the packing medium. This should be one of the important reasons that the microbial concentration and toluene removal capacity of BF1 were higher than those of BF2 in Phase II.

After Phase II, the aD_b/δ_b values of both BF1 and BF2 increased and reached about 6.0 h^{-1}. This was estimated to be caused by the increase in the specific surface area, which was a result of microbial growth and biomass accumulation. Morgan-Sagastume et al. [15] studied the physical property changes of a compost biofilter using a flow channel model, and also observed the increase in the specific surface area, especially in the inlet section of the filter bed. In this study, the specific surface area of BF2 increased, becoming close to that of BF1, which resulted in a similar microbial concentration at the end of the operation.

3.5. Pressure drops

The filter bed pressure drops is another key aspect of biofilter performance. It affects the energy consumption of the blower, which contributes most to the operation cost.

The variations of the pressure drops of the filter beds are shown in Fig. 6. Before day 130, the pressure drops of BF1 and BF2 were around 36 and 22 Pa m^{-1}, respectively. The initial pressure drop of the filter bed is mainly determined by the particles size distribution, the void fraction and the moisture content of the packing media. The pressure drop of BF2 was lower than BF1 because the void fraction of BF2 was higher than that of BF1. The pressure drops of BF1 and BF2 increased suddenly on day 24, which resulted from too much water sprayed (about 600 mL d^{-1}) due to a control error.

After day 130, the pressure drop of BF1 began to increase and remained at 300–500 Pa m^{-1}. After day 230, the pressure drop of BF1 increased significantly and the filter bed of BF1 was clogged seriously with maximum pressure drop ranging from 1000 to 2700 Pa m^{-1}. For BF2, the pressure drop jumped occasionally, reaching a maximum pressure drop of about 400 Pa m^{-1}, and came back to the initial level (20–30 Pa m^{-1}) eventually.

The pressure drop increase is an integrated result of bed compaction, biomass growth and particle agglutination [11,26]. The pressure drops of the different layers for both BF1 and BF2 were measured during the experiment and the result on day 195 is shown in Fig. 6. For BF1, only the pressure drop of the inlet layer increased significantly, while the other layer's pressure drop remained at 36 Pa m^{-1}. Since

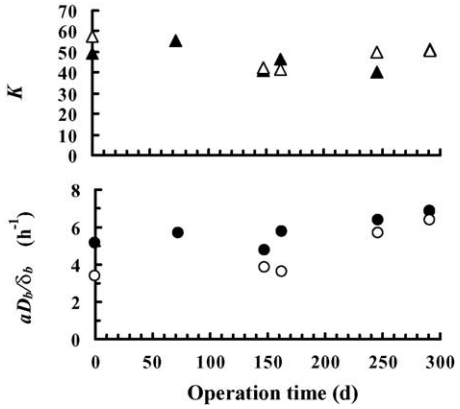

Fig. 5. Variations of the characteristic parameters of the filter beds: (▲) BF1; (△) BF2; (●) BF1 and (◯) BF2.

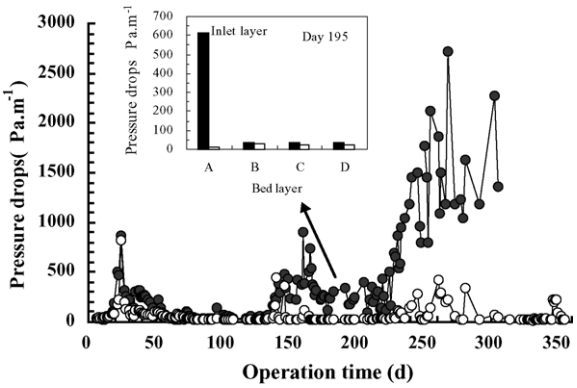

Fig. 6. Variations of the pressure drops of the filter beds and the pressure drop distribution on day 195: (●) BF1; (◯) BF2; (■) BF1 and (□) BF2.

the bed compaction occurred in each bed layer of BF1, the bed compaction was not the main reason for the pressure drop increase. The inlet layer with higher toluene concentrations usually had a higher toluene removal rate and biomass growth rate, which resulted in more biomass accumulation (see Table 2). The excess biomass blocked the flow channels in the filter bed and increased the pressure drop. This result indicated that the excess biomass accumulation contributed most to the bed clogging of BF1.

The pressure drop of BF2 was stable during the operation period, because the higher bed void fraction of BF2 reduced the likelihood of the bed clogging. The experimental results mentioned above verified that adding inert spheres into filter beds can actually lower the pressure drop and the energy consumption of the biofilter during long periods of operation.

4. Conclusions

Two biofilters packed with buckwheat hulls, one with inert spheres in the filter bed and the other without, were operated continuously for more than 300 days. The following conclusions can be drawn from the experimental results.

A comparison of the two biofilters' toluene removal efficiencies during different phases verified that it was necessary to supply enough nutrients for the biofilter to maintain its toluene removal capacity when using buckwheat hulls as the packing medium.

With sufficient nutrient feeding, the biofilter with inert spheres showed a lower toluene removal capacity in the early part of the operation due to the fact that it had a lower initial specific surface area than the biofilter without inert spheres. However, the biofilter with inert spheres had a higher toluene removal capacity in the late period of operation mainly because it had much less bed compaction than the biofilter without inert spheres.

The pressure drop of the biofilter with inert spheres was lower and more stable due to the fact that its filter bed had a large void fraction.

All the experimental results showed that adding inert spheres into the natural organic filter bed can effectively prevent bed compaction and increase the void fraction of the filter bed, which will improve the performance of the biofilter under long-term operation.

References

[1] F.I. Khan, A.K. Ghoshal, Removal of volatile organic compounds from polluted air, J. Loss Prev. Process Ind. 13 (2000) 527–545.
[2] J.W. van Groenestijn, P.G.M. Hesselink, Biotechniques for air pollution control, Biodegradation 4 (1993) 283–301.
[3] C. Kennes, F. Thalasso, Waste gas biotreatment technology, J. Chem. Technol. Biotechnol. 72 (1998) 303–319.
[4] J.E. Burgess, S.A. Parsons, R.M. Stuetz, Developments in odour control and waste gas treatment biotechnology: a review, Biotechnol. Adv. 19 (2001) 35–63.
[5] G. Leson, A.M. Winer, Biofiltration: an innovative air pollution control technology for VOC emissions, J. Air Waste Manage. Assoc. 41 (1991) 1045–1054.
[6] R.L. Corsi, L. Seed, Biofiltration of BTEX: media, substrate and loadings effects, Environ. Prog. 14 (1995) 151–158.
[7] W.J. Swanson, R.C. Loehr, Biofiltration: fundamentals, design and operations principles, and applications, J. Environ. Eng. 123 (1997) 538–546.
[8] C. Kennes, M.C. Veiga, Inert filter media for the biofiltration of waste gases-characteristics and biomass control, Rev. Environ. Sci. Biotechnol. 1 (2002) 201–214.
[9] M. Zilli, B. Fabiano, A. Ferraiolo, A. Converti, Macro-kinetic investigation on phenol uptake from air by biofiltration: influence of superficial gas flow rate and inlet pollutant concentration, Biotechnol. Bioeng. 49 (1996) 391–398.
[10] D. Arulneyam, T. Swaminathan, Biodegradation of methanol vapor in a biofilter, J. Environ. Sci. China 15 (2003) 691–696.
[11] F. Morgan-Sagastume, B.E. Sleep, D.G. Allen, Effects of biomass growth on gas pressure drop in biofilters, J. Environ. Eng. 127 (2001) 388–396.
[12] M. Delhomenie, L. Bibeau, M. Heitz, A study of the impact of particle size and adsorption phenomena in a compost-based biological filter, Chem. Eng. Sci. 57 (2002) 4999–5010.
[13] J.Y. Xi, H.Y. Hu, Y. Qian, Biological removal of gaseous toluene by a biofilter packed with buckwheat hull, in: Proceedings of the Second IWA Conference on Odor and VOCs, Singapore, 2003, session 7A.
[14] S.M. Zarook, A.A. Shaikh, S.M. Azam, Axial dispersion in biofilters, Biochem. Eng. J. 1 (1998) 77–84.
[15] J.M. Morgan-Sagastume, A. Noyola, S. Revah, S.J. Ergas, Changes in physical properties of a compost biofilter treating hydrogen sulfide, J. Air Waste Manage. Assoc. 53 (2003) 1011–1021.
[16] M.A. Garzon-Zuniga, P. Lessard, G. Buelna, Determination of the hydraulic residence time in a trickling biofilter filled with organic matter, Environ. Technol. 24 (2003) 605–614.
[17] J.A. Mendoza, O.J. Prado, M.C. Veiga, C. Kennes, Hydrodynamic behaviour and comparison of technologies for the removal of excess biomass in gas-phase biofilters, Water Res. 38 (2004) 404–413.
[18] J.Y. Xi, H.Y. Hu, H.B. Zhu, Y. Qian, The isolation and characterizations of two strains of toluene-degrading bacteria, in: Proceedings of the First National Conference on Odor Measurement and Control Techniques, Tianjin, China, 2003, pp. 72–78, written in Chinese.
[19] E. Morgenroth, E.D. Schroeder, P.Y.D. Chang, K.M. Scow, Nutrient limitation in a compost biofilter degrading hexane, J. Air Waste Manage. Assoc. 46 (1996) 300–308.
[20] O.J. Prado, J.A. Mendoza, M.C. Veiga, C. Kennes, Optimization of nutrient supply in a downflow gas-phase biofilter packed with an inert carrier, Appl. Microbiol. Biotechnol. 59 (2002) 567–573.
[21] C. Kennes, H.H.J. Cox, H.J. Doddema, W. Harder, Design and performance of biofilters for the removal of alkylbenzene vapors, J. Chem. Tech. Biotechnol. 66 (1996) 300–304.
[22] J.R. Woertz, K.A. Kinney, N.D.P. Mclntosh, P.J. Szaniszlo, Removal of toluene in a vapor-phase bioreactor containing a strain of the dimorphic black yeast *Exophiala lecanii-corni*, Biotechnol. Bioeng. 75 (2001) 550–558.
[23] D.S. Hodge, J.S. Devinny, Modeling removal of air contaminants by biofiltration, J. Environ. Eng. 121 (1995) 21–31.
[24] H.M. Tang, S.J. Hwang, S.C. Hwang, Waste gas treatment in biofilters, J. Air Waste Manage. Assoc. 46 (1996) 349–354.
[25] P.Z. Lu, C.Z. Dai, The Theory of Chromatograph, second ed., Science Press of China, Beijing, China, 1997.
[26] W.J.H. Okkerse, S.P.P. Ottengraf, B. Osinga-Kuipers, M. Okkerse, Biomass accumulation and clogging in biotrickling filters for waste gas treatment. Evaluation of a dynamic model using dichloromethane as a model pollutant, Biotechnol. Bioeng. 63 (1999) 418–430.